Production and evolution path of dileptons at HADES energies

K. Schmidt[1], E. Santini[1], S. Vogel[1], C. Sturm[2], M. Bleicher[1] and H. Stöcker[1,3,4]

[1] *Institut für Theoretische Physik, Goethe-Universität, Max-von-Laue-Str. 1, D-60438 Frankfurt am Main, Germany*

[2] *Institut für Kernphysik, Goethe-Universität, Max-von-Laue-Str. 1, D-60438 Frankfurt am Main, Germany*

[3] *Frankfurt Institute for Advanced Studies (FIAS), Ruth-Moufang-Str. 1, D-60438 Frankfurt am Main, Germany*

[4] *GSI - Helmholtzzentrum für Schwerionenforschung GmbH, Planckstrasse 1, D-64291 Darmstadt, Germany*

(Dated: December 8, 2008)

Dilepton production in intermediate energy nucleus-nucleus collisions as well as in elementary proton-proton reactions is analysed within the UrQMD transport model. For C+C collisions at 1 AGeV and 2 AGeV the resulting invariant mass spectra are compared to recent HADES data. We find that the experimental spectrum for C+C at 2 AGeV is slightly overestimated by the theoretical calculations in the region around the vector meson peak, but fairly described in the low mass region, where the data is satisfactorily saturated by the Dalitz decay of the η meson and the Δ resonance. At 1 AGeV an underestimation of the experimental data is found, pointing that at lower energies the low mass region is not fully saturated by standardly parametrized Δ Dalitz decays alone. Furthermore, predictions for dilepton spectra for *pp* reactions at 1.25 GeV, 2.2 GeV and 3.5 GeV and Ar+KCl reactions at 1.75 AGeV are presented. The study is complemented by a detailed investigation of the role of absorption of the parent particles on the corresponding dilepton yields in the regime which has so far been probed by HADES.

PACS numbers: 13.40.Hq, 24.10.Lx, 25.75.-q, 25.75.Dw

Keywords: Electromagnetic decays, Monte Carlo simulations, Relativistic heavy-ion collisions, Particle and resonance production

I. INTRODUCTION

In the last decades large experimental and theoretical efforts have been directed to the investigation of dilepton production in heavy ion collisions [1, 2, 3, 4, 5, 6, 7, 8, 9, 10, 11, 12, 13, 14, 15, 16, 17, 18, 19, 20, 21, 22, 23, 24, 25]. Dileptons represent a particularly clean and penetrating probe of the hot and dense nuclear matter due to the fact that, once produced, they essentially do

not interact with the surrounding hadronic matter. The analysis of the electromagnetic response of the dense and hot medium is tightly connected to the investigation of the in-medium modification of the vector meson properties. Vector mesons can directly decay into a lepton-antilepton pair. One therefore aims to infer information on the modifications induced by the medium on specific properties of the vector meson, such as its mass and/or its width, from the invariant mass dilepton spectra.

A first generation of ultra-relativistic heavy ion collision experiments performed in the nineties observed an enhancement of dilepton production in heavy system at low invariant mass as compared to conventional hadronic cocktails and models [1, 3]. The enhancement could be later explained by the inclusion of an in-medium modified ρ meson. At that time two possible scenarios, a dropping of the ρ meson mass according to the Brown-Rho scaling hypothesis [26] and the Hatsuda and Lee sum rule prediction [27], or a "melting" of its spectral function as expected within many-body hadronic models [8, 9, 28, 29], have been offered in attempt to explain these data [4, 5, 6, 7, 10]. If on the one side these experiments clearly showed the need for an inclusion of in-medium effects, on the other side it could not be decided, on the basis of the experimental data, whether the additional strength at lower invariant masses was due to a dropping of the vector meson mass or to the broadening of its spectral function. A first answer in this direction came from the measurements performed by the NA60 Collaboration [15]. The data strongly favour the broadening over the dropping mass scenario. A similar conclusion is suggested by recent higher resolution CERES data [16].

At lower bombarding energies dileptons have been measured by the DLS Collaboration at BEVELAC [11]. The most striking result of the DLS experiment was an observed enhancement at lower invariant masses in nucleus-nucleus collisions at 1 AGeV with respect to the corresponding theoretical spectra resulting from transport calculations [12, 13, 14]. Differently to the ultra-relativistic case, none of the in-medium scenarios which had successfully explained the ultra-relativistic heavy ion collision data could account for the observed enhancement [12, 13] (this is known as the DLS puzzle). In the meanwhile the HADES spectrometer has been built at GSI with the aim of performing a systematic study of dilepton production in elementary, as well as heavy ion reactions. First HADES data have recently been presented [17, 18], accompanied by a growing related theoretical activity [19, 20, 21, 23, 25].

Aim of this work is a detailed investigation of dilepton production in heavy ion and elementary reactions at SIS energies. The analysis is performed within the microscopic UrQMD model, a non-equilibrium transport approach based on the quantum molecular dynamics concept [30, 31, 32]. The model allows for the production of all established meson and baryon resonances up to

about 2 GeV with all corresponding isospin projections and antiparticle-states. The collision term describes particle production by resonant excitation channels and, for higher energies, within a string fragmentation scheme. For dilepton production at SIS energies, the resonant production of neutral mesons is most important. The model allows to study the full space time evolution for all hadrons, resonances and their decay products. This permits to explore the emission patterns of the resonances in detail and to gain insight into the origin of the resonances. UrQMD has been successfully applied to study light and heavy ion reactions at SIS. Detailed comparisons of UrQMD with a large body of experimental data at SIS energies can be found in [33]. For further details of the model the reader is referred to [34, 35], the latest version (v2.3) is described in [36].

The systems analysed here have been chosen according to the HADES program. For those systems for which the HADES data and detector filter function are available a direct comparison to the data is performed. The additional calculations are given as predictions which can be compared to experimental data in the near future. The outline of the paper is the following: After a brief survey of the UrQMD model and of the therein implemented dilepton production channels in Section II, proton-proton reactions are discussed in Section III, where the model calculations are compared to existing DLS data and predictions for the related projects of the HADES Collaboration, *pp* at 1.25 GeV, 2.2 GeV and 3.5 GeV, are presented. In Section IV dilepton spectra for C+C collisions are shown. In Section V we turn to predictions for the forthcoming analysis of dilepton production in Ar+KCl collisions . Section VI is devoted to the study of the time evolution of the dilepton emission and its connection with the various density regimes experienced in the course of the heavy ion collision. Summary and concluding remarks are finally given in Section VII.

II. THE MODEL

A. Meson production in UrQMD

In the UrQMD model the formation of light mesons at low energies is modelled as a multi-step process that proceeds via intermediate heavy baryon and meson resonances and their subsequent decay [37]. The resonance parameters (pole masses, widths and branching ratios) are within the limits of [38]. A comparison between the exclusive and inclusive cross sections for the production of neutral $\pi^0, \eta, \rho^0, \omega$ mesons in *pp* reactions obtained within the UrQMD model and experimental data can be found in [35]. The resonant exclusive production of the ρ^0 meson, particularly important at low energies, will be discussed more in detail in Section IV A.

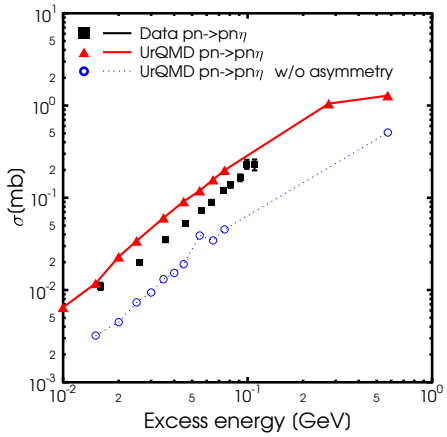

FIG. 1: (Color online) The η production cross section from pn reactions as a function of the excess energy. The UrQMD results obtained with the novel introduction of the isospin asymmetry in the η production cross section (triangles) are compared to experimental data [40]. The circles refer to calculations which neglect such asymmetry and are shown for completeness.

In the analysis of dilepton spectra in nucleus-nucleus collisions performed with the UrQMD model in [13], the dilepton yield originating from the η Dalitz decay was found about a factor two lower than in Ref. [12] and Ref. [39]. In the latter, the η channel had been determined from the measurements of the TAPS Collaboration. As already anticipated in [13], the discrepancy could be attributable to the fact that the asymmetry in the η production in pp and pn reactions (η production cross sections in pn reactions are about a factor five higher than in pp reaction) had been neglected in the calculations. Such asymmetry has been introduced for the present analysis (see Fig. 1). The inclusion has been performed, as in [41], at the level of the production cross section of the $N^{\star}(1535)$ resonance. For the C+C reactions under study the η multiplicity obtained within the UrQMD model is now consistent with the value measured by the TAPS Collaboration [42], as shown in Fig. 2. The experimental constraint imposed by the TAPS measurements on the η Dalitz contribution to the dilepton spectra in nucleus-nucleus collisions is thus respected by our calculations. Especially for C+C collisions at 2 AGeV, this is very important since, as we will see, the η decay plays an important role in determining the spectra in the low mass region.

The energy dependence of the exclusive $pn \rightarrow pn\eta$ cross section as shown in Fig. 1 provides a reasonable description of the data, however a finer parametrization, as e.g. in Ref. [23], might be required in future studies of dilepton production in elementary pn reactions. Especially for those cases where fixing the η contribution with high precision is mandatory in order to achieve

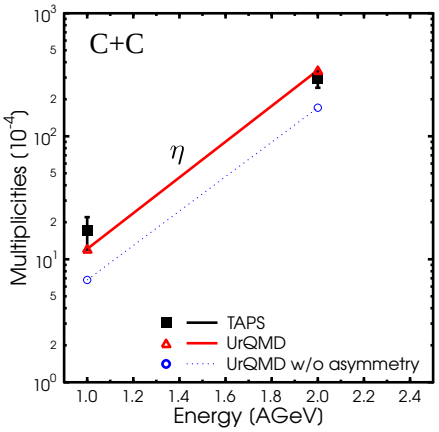

FIG. 2: (Color online) Average η multiplicity in C+C reactions at 1 AGeV and 2 AGeV from UrQMD (triangle) in comparison to the values reported by the TAPS Collaboration [42]. The circles refer to the standard calculations which neglect the isospin asymmetry in the η production cross section and are shown for completeness.

an unique interpretation of the experimental data in the low mass region a re-tuning is necessary. However, *pn* reactions are not the major subject of this work, and the new prescription used here for the treatment of η production provides sufficient robustness for the dilepton studies presented in the next sections.

B. Dilepton radiation in UrQMD

In UrQMD, dilepton pairs are generated from the mesonic Dalitz decays $\pi^0 \to \gamma e^+e^-$, $\eta \to \gamma e^+e^-$, $\eta' \to \gamma e^+e^-$ and $\omega \to \pi^0 e^+e^-$, the direct decay of the ρ, ω and ϕ vector mesons and the Dalitz decay of the Δ resonance.

Decays of the form, with P being a pseudoscalar meson and V a vector meson,

$$P \to \gamma e^+e^-, V \to Pe^+e^- \tag{1}$$

can be decomposed into the corresponding decays into a virtual photon $\gamma^\star$, $P \to \gamma\gamma^\star$, $V \to P\gamma^\star$, and the subsequent decay of the photon via electromagnetic conversion, $\gamma^\star \to e^+e^-$ [43, 44, 45]:

$$\frac{d\Gamma_{P\to\gamma e^+e^-}}{dM^2} = \Gamma_{P\to\gamma\gamma^\star}\,\frac{1}{\pi M^4}\,M\Gamma_{\gamma^\star\to e^+e^-}\ , \tag{2}$$

$$\frac{d\Gamma_{V\to Pe^+e^-}}{dM^2} = \Gamma_{V\to P\gamma^\star}\,\frac{1}{\pi M^4}\,M\Gamma_{\gamma^\star\to e^+e^-}\ , \tag{3}$$

where M is the mass of the virtual photon or, equivalently, the invariant mass of the lepton pair. The internal conversion probability of the photon is given by:

$$M\Gamma_{\gamma^\star\to e^+e^-} = \frac{\alpha}{3}\,M^2\,\sqrt{1-\frac{4m_e^2}{M^2}}\left(1+\frac{2m_e^2}{M^2}\right) \tag{4}$$

with m_e being the electron mass. The widths $\Gamma_{P\to\gamma\gamma^\star}$ and $\Gamma_{V\to P\gamma^\star}$ can be related to the corresponding radiative widths $\Gamma_{P\to 2\gamma}$ and $\Gamma_{V\to P\gamma}$:

$$\Gamma_{P\to\gamma\gamma^\star} \;=\; 2\,\Gamma_{P\to 2\gamma}\left(1-\frac{M^2}{m_P^2}\right)^3 |F_{P\gamma\gamma^\star}(M^2)|^2, \tag{5}$$

$$\Gamma_{V\to P\gamma^\star} \;=\; \Gamma_{V\to P\gamma}\left[\left(1+\frac{M^2}{m_V^2-m_P^2}\right)^2-\left(\frac{2m_V M}{m_V^2-m_P^2}\right)^2\right]^{3/2} |F_{VP\gamma^\star}(M^2)|^2, \tag{6}$$

where m_P and m_V are the masses of the pseudoscalar and vector meson respectively and $F_{P\gamma\gamma^\star}(M^2)$, $F_{VP\gamma^\star}(M^2)$ denote the form factors with $F_{P\gamma\gamma^\star}(0) = F_{VP\gamma^\star}(0) = 1$. The factor 2 in (5) occurs due to the identity of the two photons in the $P\to 2\gamma$ decay. The form factors can be obtained from the vector meson dominance model (VMD). In the present calculations the following parametrisations are employed [7, 43]:

$$\begin{aligned}
F_{\pi^0}(M^2) &= 1+b_{\pi^0}M^2,\\
F_{\eta}(M^2) &= \left(1-\frac{M^2}{\Lambda_\eta^2}\right)^{-1},\\
\left|F_{\omega}(M^2)\right|^2 &= \frac{\Lambda_\omega^2(\Lambda_\omega^2+\gamma_\omega^2)}{(\Lambda_\omega^2-M^2)^2+\Lambda_\omega^2\gamma_\omega^2},\\
\left|F_{\eta'}(M^2)\right|^2 &= \frac{\Lambda_{\eta'}^2(\Lambda_{\eta'}^2+\gamma_{\eta'}^2)}{(\Lambda_{\eta'}^2-M^2)^2+\Lambda_{\eta'}^2\gamma_{\eta'}^2}
\end{aligned} \tag{7}$$

with $b_{\pi^0} = 5.5\,\mathrm{GeV}^{-2}$, $\Lambda_\eta = 0.72\,\mathrm{GeV}$, $\Lambda_\omega = 0.65\,\mathrm{GeV}$, $\gamma_\omega = 0.04\,\mathrm{GeV}$, $\Lambda_{\eta'} = 0.76\,\mathrm{GeV}$ and $\gamma'_\eta = 0.10\,\mathrm{GeV}$. In (7) the abbreviations F_P and F_V have been used to denote respectively $F_{P\gamma\gamma^\star}$ and $F_{VP\gamma^\star}$.

The width for the direct decay of a vector meson $V = \rho^0,\ \omega,\ \phi$ to a dilepton pair varies with the dilepton mass like M^{-3} according to [7]:

$$\Gamma_{V\to e^+e^-}(M) = \frac{\Gamma_{V\to e^+e^-}(m_V)}{m_V}\frac{m_V^4}{M^3}\sqrt{1-\frac{4m_e^2}{M^2}}\left(1+\frac{2m_e^2}{M^2}\right) \tag{8}$$

with $\Gamma_{V\to e^+e^-}(m_V)$ being the partial decay width at the meson pole mass.

The decomposition of the $\Delta\to Ne^+e^-$ decay into the $\Delta\to N\gamma^\star$ decay and subsequent conversion of the photon leads to the following expression for the differential decay width:

$$\frac{d\Gamma_{\Delta\to Ne^+e^-}}{dM^2} = \frac{\alpha}{3\pi M^2}\Gamma_{\Delta\to N\gamma^\star}\ . \tag{9}$$

Here the electron mass has been neglected. The decay width into a massive photon reads [46]:

$$\Gamma_{\Delta\to N\gamma^\star}(M_\Delta, M) = \frac{\lambda^{1/2}(M^2, m_N^2, M_\Delta^2)}{16\pi M_\Delta^2} m_N \times \left[2\mathcal{M}_t(M, M_\Delta) + \mathcal{M}_l(M, M_\Delta)\right] , \tag{10}$$

where the kinematic function λ is defined by $\lambda(m_A^2, m_1^2, m_2^2) = (m_A^2 - (m_1+m_2)^2)(m_A^2 - (m_1-m_2)^2)$ and M_Δ is the resonance running mass. The matrix elements $\mathcal{M}_t$ and $\mathcal{M}_l$ are taken from [46]. The coupling constant g appearing in the expression for $\mathcal{M}_t$ and $\mathcal{M}_l$ has been chosen as $g = 5.44$, in order to reproduce the value of the radiative decay width, as done e.g. in [47].

C. Shining method

The "shining" method (also called time integration method) was introduced in [48] and [2] and assumes that a resonance can continuously emit dileptons over its whole lifetime. The dilepton yield is obtained by integration of the dilepton emission rate over time, taking the collisional broadening of each individual parent resonance into account:

$$\frac{dN_{e^+e^-}}{dM} = \frac{\Delta N_{e^+e^-}}{\Delta M} = \sum_{j=1}^{N_{\Delta M}} \int_{t_i^j}^{t_f^j} \frac{dt}{\gamma} \frac{\Gamma_{e^+e^-}(M)}{\Delta M} \tag{11}$$

Here $\Gamma_{e^+e^-}(M)$ is the electromagnetic decay width of the considered resonance defined in (8–10) and $t = t_i$ (t_f) the time at which the resonance appeared in (disappeared from) the system. For the calculations applying the "shining" method the whole time evolution of the collision is reconstructed. Each resonance is followed from the production time t_i to a final time t_f at which the resonance decays or is reabsorbed. We implement the shining method for the short-lived vector mesons ρ and ω and the baryonic resonance Δ.

In an alternative method, dileptons have been extracted at the point of decay of the resonances [20]. The dilepton yield is calculated at the decay vertex from the branching ratio. Thus, in this method the contribution to the dilepton yield of the reabsorbed resonances is neglected. As shown in [24] this contribution is however small. A comparison between the two methods is realised in the next section.

III. ELEMENTARY REACTIONS

A. Comparison to DLS measurements

Before addressing heavy ion collisions we consider dilepton production in elementary reactions. The latter are very important to gain a better understanding of the various processes contributing to the dilepton production and of their relative weights. In the energy range of interest for this work there exist measurements from the DLS [49] and HADES Collaboration.

Differential dilepton cross sections have been calculated with the present model for pp reactions at beam energies of 1.04, 1.27, 1.61, 1.85 , 2.09 and 4.88 GeV. The results are presented in Fig. 3 in comparison to the DLS data [49]. In order to perform the comparison, the DLS acceptance filter and mass resolution have been included. For collisions at 1.04–2.09 GeV the agreement with the available data is generally reasonable in the region $M \leq 0.45$ GeV, where the π^0, Δ and η Dalitz decays dominate, a systematic overestimation of the data is observed at higher masses. Especially at 2.09 GeV a clear overestimation of the dilepton cross section around the vector meson peak is present, a result which is analogous to the findings of Ref. [23]. This might be due to an insufficient modelling of the production rate of high mass resonances in $pp \to pN^*$, $pp \to p\Delta^*$ collisions. We investigate this effect more in detail in Section IV A. At bombarding energy of 4.88 GeV an inversion of this trend is observed and data are underestimated by the model calculations in the low invariant mass region but good described in the vector meson region. This is not a contradiction. The main difference lies in the fact that at 4.88 GeV the exclusive production of the ρ meson does not affect significantly the inclusive production. The latter, on the other side, determines the ρ meson yields in the reactions at 1.04–2.9 GeV.

B. Predictions for HADES

The HADES physic program includes measurement of pp reactions at 1.25 GeV, 2.2 GeV and 3.5 GeV which we want to discuss here. In Fig. 4, UrQMD calculations for the three energies are presented. The beam energy $E = 1.25$ GeV is below the $pp \to pp\eta$ threshold and is therefore optimal for studying the contribution from Δ Dalitz. For $M > 0.45$ GeV a noticeable contribution from $\rho^0 \to e^+e^-$ is visible. This result differs from other calculations [23], where the contribution from the direct decay of the ρ meson is not seen at the lowest energy. This is due to the omission of an explicit treatment of ρ meson production via resonant mechanism in [23], where a simplified parametrization of the $pp \to \rho X$ (vacuum) cross section of the

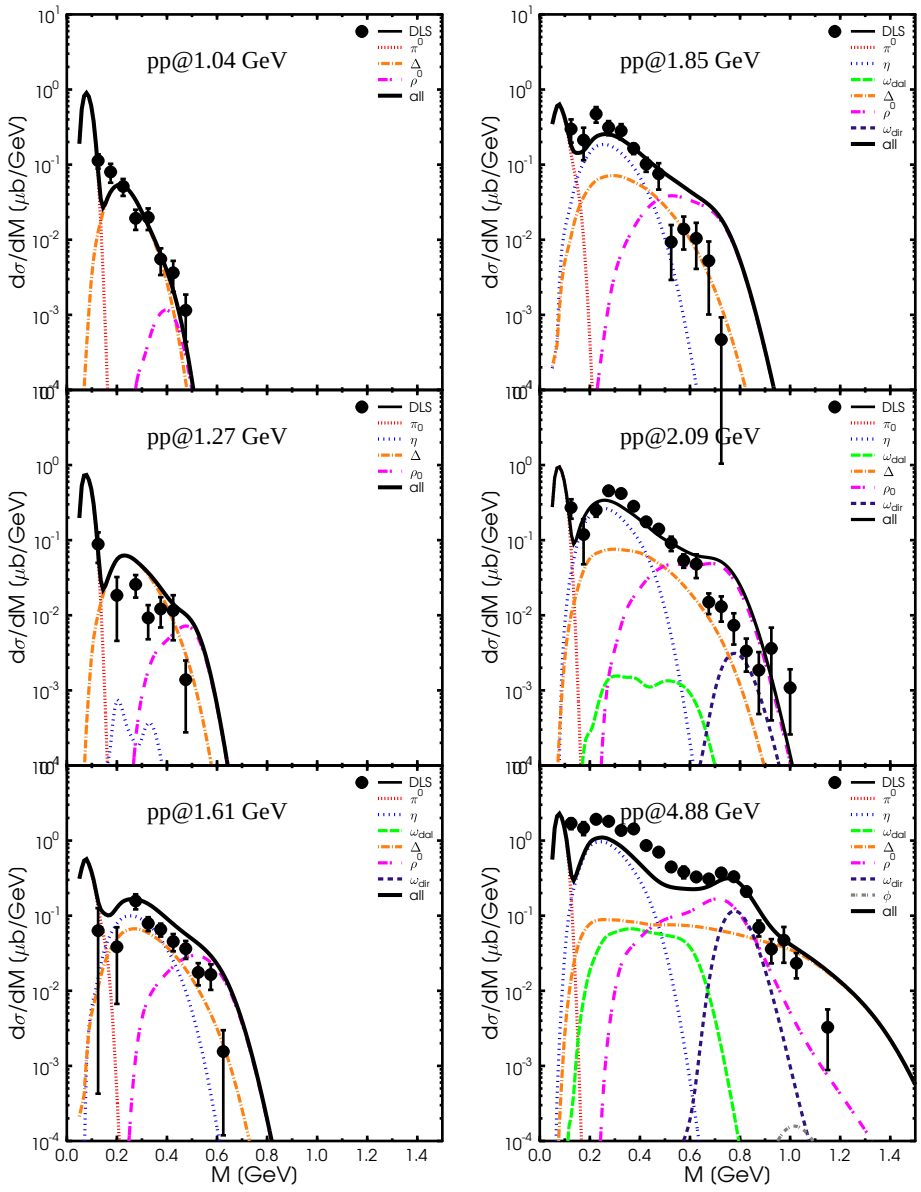

FIG. 3: (Color online) UrQMD model calculations for dilepton spectra from *pp* reactions at 1.04, 1.27, 1.61, 1.85 , 2.09 and 4.88 GeV in comparison to the DLS data [49], including the DLS acceptance filter and mass resolution. The different color lines display individual channels in the transport calculation, as indicated in the legend.

form $\sigma(pp \to \rho X) \sim \int 2.2\ (\frac{s}{s_0(M)} - 1)^{1.47}\ (\frac{s}{s_0(M)})^{-1.1}\ A(M)\ dM$ has been employed. Here $A(M)$ denotes the meson spectral function and the integration is performed within the appropriate kinematical limits. Close to the physical threshold for ρ meson production, $\sqrt{s}_{\rm th} = 2m_N + 2m_\pi$, such omission results in smaller values of the cross section than those of this work (see Section IV A) and of other resonance model based approaches (see e.g. [14, 41, 50]). In our model, this contribu-

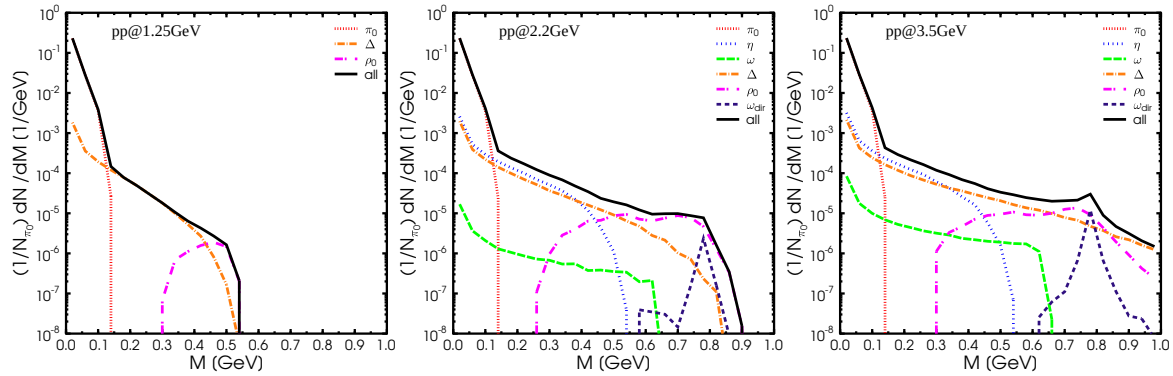

FIG. 4: (Color online) UrQMD model calculations for dilepton spectra from p+p collisions at beam energies of 1.25 GeV (left panel), 2.2 GeV (middle panel) and 3.5 GeV (right part). The different color lines display individual channels from the transport calculation, as indicated in the legend.

tion arises naturally due to the possibility for baryonic resonances to decay into ρ. At rather low energies, this leads to the emission of a ρ meson with a mass distribution strongly biased by energy constraints. Here, the ρ mesons originates in particular from the decay of the $N^*(1520)$ resonance. For this chain the threshold is only $M = 2m_\pi$ and not $m_\rho^{\rm pole}$. Early investigations on the role of the $N^*(1520)$ resonance for subthreshold ρ meson production were performed in Refs. [47, 51].

For higher beam energies all decays are possible as for the nucleus nucleus system. Both for 2.2 GeV and 3.5 GeV the dilepton spectra in the lower mass regime are dominated by the long-lived resonances and the Δ resonance. For higher masses the direct decay of the ρ meson becomes more important and the double peak shape of the e^+e^--pairs originating from ρ is visible. At a beam energy of 3.5 GeV the contribution from the direct ω decay leads to a visible peak in the dilepton spectrum at $M \approx 0.8$ GeV.

IV. DILEPTON YIELDS IN C+C COLLISIONS

In this Section we present calculations for dilepton spectra in minimum bias C+C reactions at 1.0 AGeV and 2.0 AGeV and compare them to the data resulting from the measurements performed by the HADES Collaboration [17, 18]. In order to make the comparison with the experimental data, the filter function provided by the HADES Collaboration has been implemented [17, 18]. In agreement with the treatment of the experimental data, dilepton events with opening angle $\Theta_{e^+e^-} \leq 9^\circ$ have been rejected and the spectra have been normalised to the mean π^0 multiplicity.

We first discuss the results obtained applying the "shining" method for the extraction of the dilepton yield and address Fig. 5, where the contributions to the spectra of the different channels are additionally explicitly shown. Both spectra are dominated by the π^0 decay for invariant masses $M \leq m_\pi$.

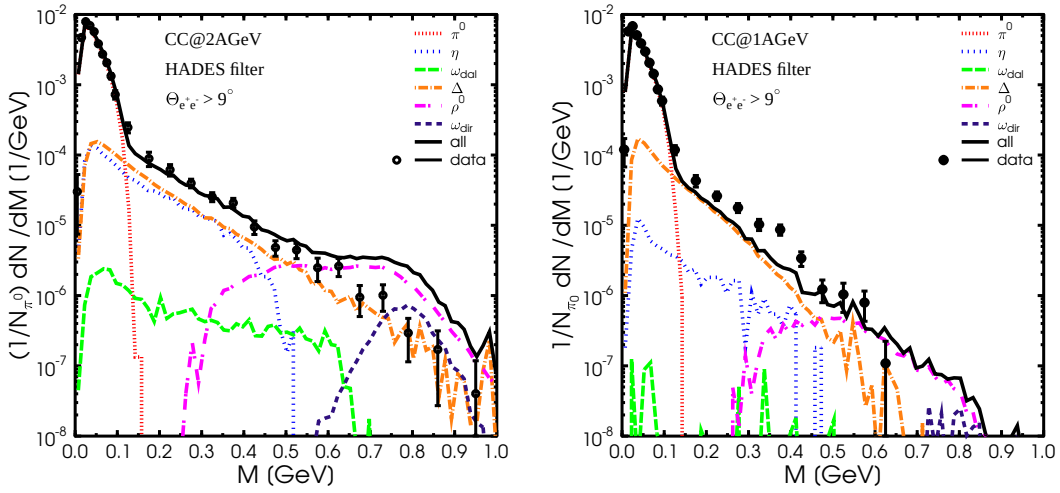

FIG. 5: (Color online) UrQMD model calculations for dilepton spectra from C+C collisions at beam energies of 2 AGeV (left) and 1 AGeV (right) in comparison to HADES data [17]. The different color lines display individual channels in the transport calculation, as indicated in the legend.

In the case of C+C at 2 AGeV the η and Δ Dalitz decays dominate for $m_\pi \leq M \leq 0.5$ GeV with comparable magnitude. The present result for the Δ Dalitz contribution to the spectra is quantitatively similar to the result of Ref. [23] , whereas in [21] and [25] a smaller contribution was found. The direct decay of the ρ meson start to play a sizable role for $M \geq 0.5$ GeV. Due to the rapid decrease of the Δ Dalitz contribution, the relative importance of the ρ meson direct decay channel grows with increasing invariant mass, from being at first comparable to the Δ Dalitz to becoming the dominant contribution in the region of the vector meson peak. The low invariant mass region of the spectrum ($M < 0.5$ GeV) is successfully described by the UrQMD calculations. However, an overestimation of the data is observed at higher masses. A qualitatively analogous result has been found in the analysis of [23], were the "vacuum" calculation for C+C at 2 AGeV resulted in an overestimation of the data in the region of the vector meson peak. However, the enhancement being more localised around the peak than in our case and about a factor 1.5 lower at $M \sim m_{peak}$. The difference lies in the contribution originating from the direct ρ meson decay,

suggesting a probably different value of ρ meson multiplicity.

The spectrum obtained assuming that dileptons are emitted at the decay vertex of the parent resonance is shown in Fig. 6 and compared to the result of Fig. 5. The two results present no sizable differences, indicating that the methods to extract dileptons are essentially equivalent when looking at time integrated yields at low energies. The reason for that lies in the smallness of the yield originating from reabsorbed resonances if compared to the emission from decaying resonances [24]. The effect of absorption processes on the dilepton spectrum is analysed in the Section VI.

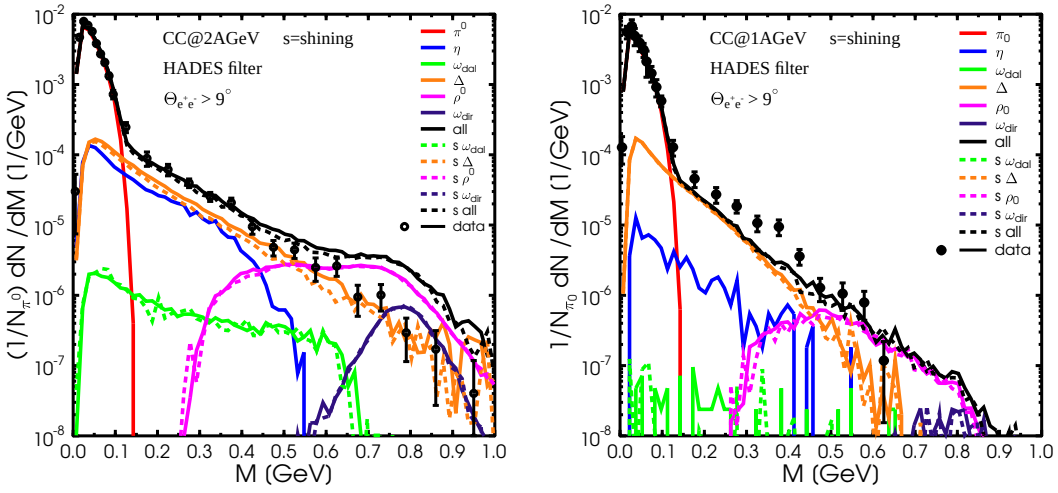

FIG. 6: (Color online) UrQMD model calculations for dilepton spectra from C+C collisions at beam energies of 2 AGeV (left) and 1 AGeV (right) in comparison to HADES data [17]. The full lines correspond to determination of the dilepton yield at the decay vertex of the parent particle. The dashed lines correspond to the dilepton yield resulting from the application of the shining method. The different color lines display individual channels in the transport calculation, as indicated in the legend, with s indicating the shining method.

Unfortunately no inclusive data on ρ meson production cross section are available at the energy interesting for this work. Whether the here observed overestimation of the HADES data is due to an overestimation of the ρ meson multiplicities from the nucleon-nucleon collisions or to a more complex in-medium mechanism, or both, cannot be decided on the basis of this experimental data. A comparison of the mass differential dilepton cross section for pp reactions to existing DLS data has been performed and discussed in the previous section. The analysis suggested that the meson multiplicity might be indeed slightly overshot. Due to the low resolution of the DLS data, it is for the moment not possible to make exact quantitative conclusions. Nevertheless, an attempt

to estimate possible model incertainties and their consequences is made in the next section. In this respect, the forthcoming HADES data on dilepton production in elementary reactions will be extremely helpful to indirectly constrain vector meson multiplicities.

At 1 AGeV a systematic underestimation of the data is observed in the mass region $0.2 < M < 0.4$ GeV with a maximum discrepancy at $M \approx 0.38$ GeV. The result is qualitatively in line with previous investigations of dilepton production in 1 AGeV nucleus-nucleus collisions which link back in time to the DLS era [12, 13, 14]. Quantitatively, however, the discrepancy between the theoretical and experimental spectra spans here between a factor 1.5 and 2 from $M = 0.225$ GeV to $M = 0.325$ and is then at most of a factor 3 at $M = 0.375$ GeV, whereas discrepancies of a factor four had emerged from the studies performed in the nineties [12, 13]. Enhanced bremsstrahlung cross sections in line with one boson exchange calculations by Kaptari and Kämpfer [52] have been recently proposed as possible explanation of the DLS puzzle [23]. The issue is however quite controversial. For *pn* reactions the cross sections of Ref. [52] differ up to a factor four from previous calculations [53, 54]. In [52] and [54] the same couplings have been used, but differences can originate due to a different prescription used by the groups to restore gauge invariance in the effective theory. Since the way this restoration can be achieved is not unique, there are no straight arguments which favor one calculation over the other. To investigate this discrepancy, dilepton production in nucleon-nucleon collisions has been recently revisited within a fully relativistic and gauge invariant framework [55]. For the various contributions analyzed –*pp* bremsstrahlung, *pn* bremsstrahlung, as well as contributions with the Δ isobar intermediate state– the authors of [55] found cross sections smaller than those in Ref. [52]. In *pn* collisions at beam energies of 1.04 and 2.09 GeV, in particular, differences in the bremsstrahlung contribution by factors ranging between 2 and 3 were foud. Future HADES measurements of dilepton spectra in elementary, especially *pn*, collisions will help to shed light into this new puzzle.

A. Discussion

The comparison with DLS data for dilepton production in *pp* collisions suggested that at the lowest energies (1.04-2.09 GeV) the ρ meson yield might be overestimated by our model. Figure 7 shows the cross sections for the inclusive ($pp \to \rho^0 X$) and exclusive ($pp \to pp\rho^0$) production of the neutral ρ meson in *pp* collisions, in comparison with experimental data from Ref. [56]. The points corresponding to the energies scanned by the DLS *pp* program are labelled by the corresponding laboratory energies to simplify the readability of the figure. The resonant contribution to the ex-

clusive production, important at the energies relevant for this work, is separately shown. Moreover, the contribution of the most important resonances is explicitly shown. To specify the order of the relative scale, the contribution of some of the less important resonance is shown too. The full list of resonances which couple to the ρ meson in the UrQMD model is given in Table I together with the values of the respective branching ratios in the $N\rho$ decay channel as used in UrQMD v2.3. Some of the values for the branching ratios differ from the ones used in UrQMD v1.0 [13, 34]. However, the same values are used since UrQMD v1.1. Above the threshold for meson production by string fragmentation and decay, the $pp \rightarrow pp\rho^0$ reaction channel is additionally populated by processes involving strings.

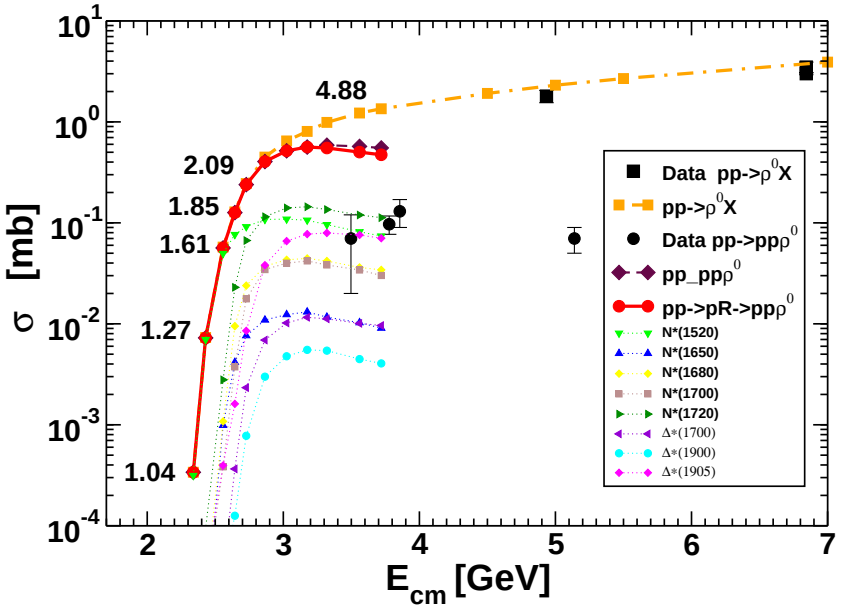

FIG. 7: (Color online) Cross sections for ρ^0 meson production in pp collisions. Calculations are shown for inclusive ($pp \rightarrow \rho^0 X$) and exclusive ($pp \rightarrow pp\rho^0$) in comparison to experimental data [56]. The contribution of the most important resonances to the resonant exclusive production is additionally shown.

Unless explicitly specified, in the following we will discuss in terms of laboratory energies. One observes that in collisions at laboratory energies of 1.04-2.09 GeV the ρ meson production is determined by the excitation of Δ^* and N^* resonances in reactions $pp \rightarrow pN^*$ and $pp \rightarrow p\Delta^*$ and the inclusive production of the ρ meson coincides with the exclusive production. In particular, the latter is practically saturated by the contribution of the $N^*(1520)$ resonance up to beam energies of 1.61 GeV. On the contrary, at 4.88 GeV, the inclusive production dominates by far the exclusive production. The first datapoints on inclusive production are well reproduced by the model, but are far away from the energies spanned by the DLS and the HADES experiments. The exclusive

TABLE I: List of the non strange resonances included in UrQMD with non vanishing branching ratio into the $N\rho$ decay channel.

Resonance	Br($N\rho$)	Resonance	Br($N\rho$)
$N^*(1520)$	.15	$\Delta^*(1620)$	.05
$N^*(1650)$	.06	$\Delta^*(1700)$	.25
$N^*(1680)$	.10	$\Delta^*(1900)$	.25
$N^*(1700)$	.20	$\Delta^*(1905)$	.80
$N^*(1710)$	.05	$\Delta^*(1910)$	.10
$N^*(1720)$	.73	$\Delta^*(1930)$	.22
$N^*(1900)$	.15	$\Delta^*(1950)$	.08
$N^*(1990)$	.43		
$N^*(2080)$	.12		
$N^*(2190)$	.24		
$N^*(2220)$	.22		
$N^*(2250)$	.25		

production, on the contrary, is systematically overestimated.

Poor and often contradictory experimental information is available on the production cross sections of N^* and Δ^* resonances. For example, in the case of the $N^*(1520)$ resonance a reduction of the cross section currently used in UrQMD by a factor 3 is possible in comparison to the experimental data [56] and results even in a smaller value of the weighted least mean square. For this reason, we investigated the effect that an eventual overestimation of the $pp \to p\Delta^*$ and $pp \to pN^*$ cross sections would have on the ρ^0 meson and, consequently, dilepton production. Due to the lack of high quality data and to explore the effects of this change, we divide all $pp \to p\Delta^*$ and $pp \to pN^*$ cross sections by a factor 3 with exception for the $pp \to pN^*(1535)$ cross section which is constrained by the η production. This procedure is surely too crude, but provides a rough estimate of the consequences that an eventual insufficient modelling of the hitherto used $pp \to p\Delta^*$ and $pp \to pN^*$ cross sections might have on the model calculations for dilepton spectra. The results obtained with the modified values of the $pp \to p\Delta^*$ and $pp \to pN^*$ cross sections are shown in Fig. 8 and Fig. 9. We observe that the model calculations of the exclusive ρ^0 meson production cross sections moves closer to the experimental data and the DLS data are well described in all mass range. In particular, the peak previously observed in the dilepton spectra for pp collisions at 2.09 GeV vanishes to a large extent. We notice that the readjustment of the exclusive production of the ρ^0 meson does not alter the inclusive production at laboratory energy of 4.88 GeV, neither

the respective result for the dilepton spectra.

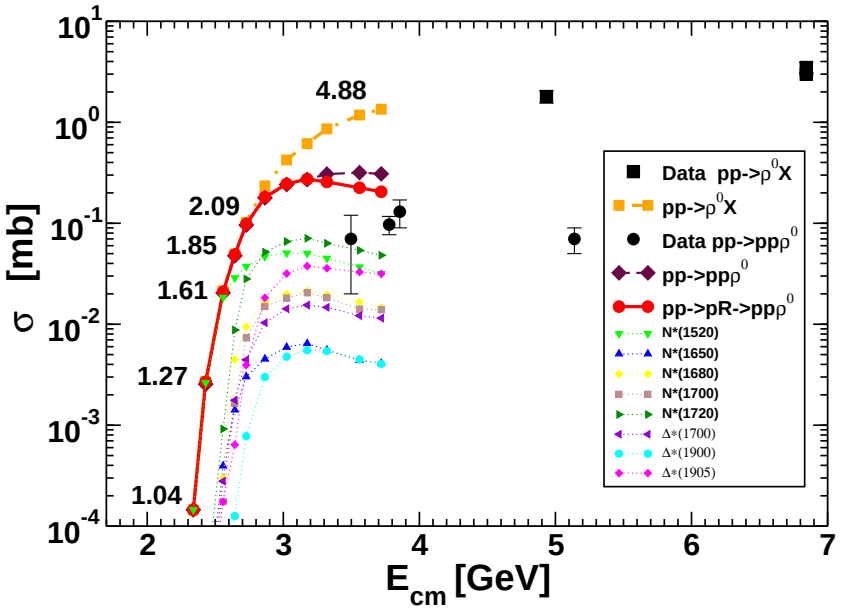

FIG. 8: (Color online) Same as Fig. 7, but for a smaller value of the $pp \to p\Delta^*$ and $pp \to pN^*$ cross sections, as explained in the text.

However, the main features of our results remain. In particular, the contribution to the dilepton spectrum from ρ^0 mesons at the lowest energies, although reduced, is still visible and distinguishable. Concerning the reaction C+C at 2 AGeV, we observe that the HADES data remain overestimated in the peak region even when the readjusted cross sections are used, as shown in Fig. 10. Many processes, such as multiple scattering, backwards reactions, Fermi motion, etc... distinguish a heavy ion collision from a simple superposition of elementary reactions occurring at the same beam energy. It is also clear that in the local equilibrium limit particle production would be statistical and information on the employed elementary cross sections would be lost. In the present case, which can be seen as an intermediate regime between the two limiting cases of an elementary reaction and an equilibrated system, we find that a small readjustment of some particular cross sections can still affect the dilepton spectrum, but differences are smaller than in the elementary case.

V. PREDICTIONS FOR AR+KCL

In this section we consider the reaction Ar+KCl at 1.75 AGeV, recently measured and currently analyzed by the HADES Collaboration. The predictions presented here refer to minimum bias

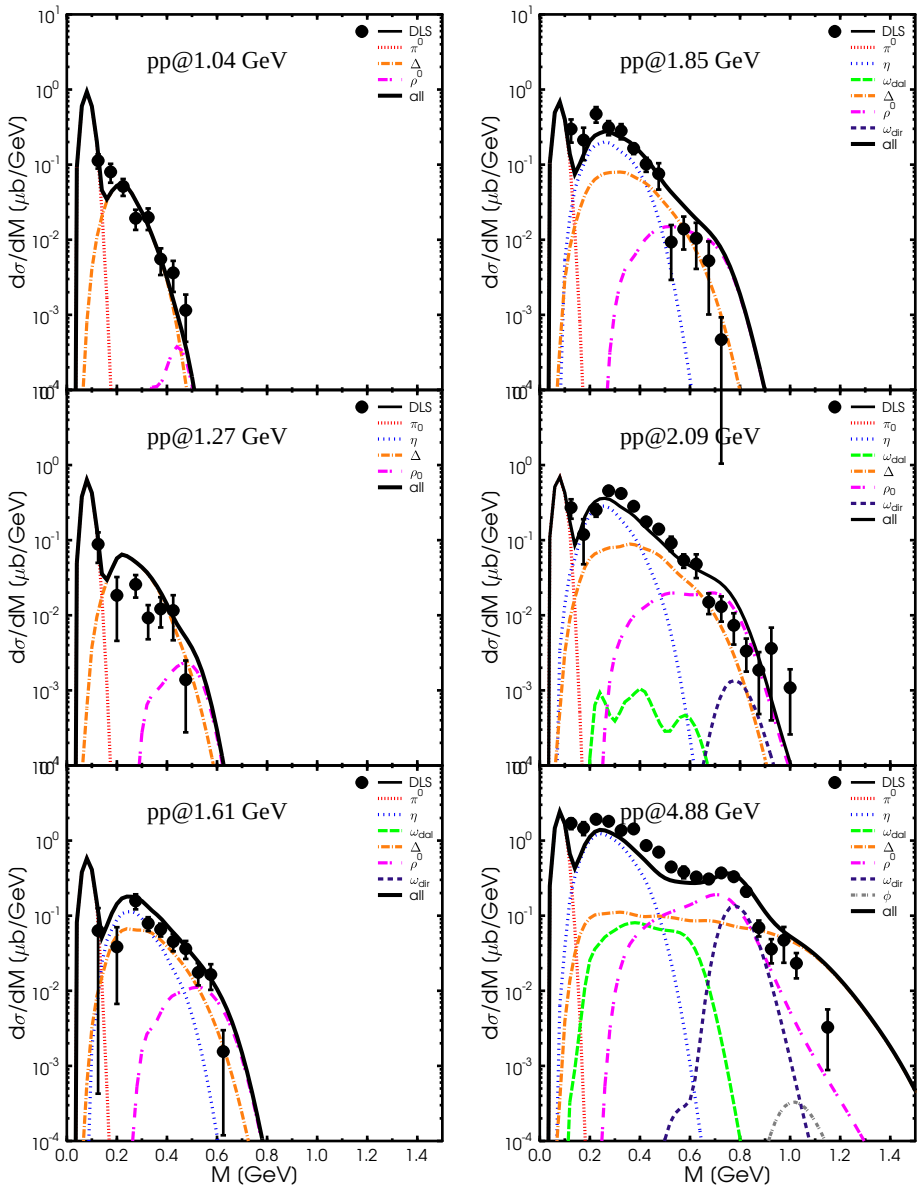

FIG. 9: (Color online) Same as Fig. 3, but for a smaller value of the $pp \to p\Delta^*$ and $pp \to pN^*$ cross sections.

calculations and have been obtained adopting the shining method. All spectra are normalised to the pion multiplicity.

The invariant mass differential dilepton spectrum is shown in Fig.11. Compared to C+C at 2 AGeV we observe a smaller contribution of the η resonances relatively to the e^+e^--pairs originating from the Δ Dalitz decay. Up to a dilepton mass of 0.4 GeV the biggest contribution to this mass spectrum occurs from the long-lived mesons η and π^0 and the baryonic resonance Δ. Considering the contribution originating from vector mesons it is visible that the ω Dalitz decay again plays only a subordinate role, while the e^+e^--pair production from ω direct decay becomes

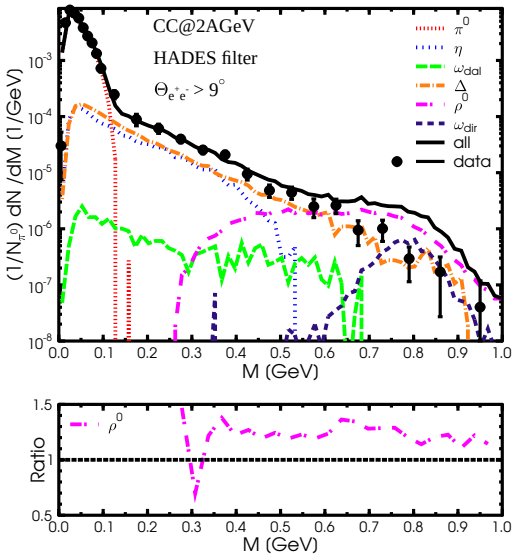

FIG. 10: (Color online) Upper panel: Same as Fig. 5, but for a smaller value of the $pp \to p\Delta^*$ and $pp \to pN^*$ cross sections. Lower panel: Ratio between the ρ^0 contribution to the dilepton spectra of Fig. 5 and Fig. 10.

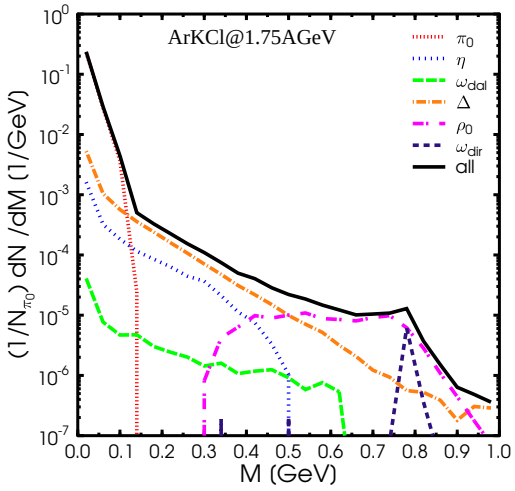

FIG. 11: (Color online) UrQMD model calculations for dilepton invariant mass spectra from Ar+KCl collisions at beam energy of 1.75 AGeV. The calculations were performed with the shining method.

important for higher invariant mass, such that in the (unfiltered) dilepton spectrum a peak at $M \approx 0.8$ GeV is visible. The direct decay of the vector meson ρ dominates the mass spectrum for $M > 0.5$ GeV.

VI. TRACING THE DILEPTON EMISSION BACK IN TIME

In this section we investigate the dependence of the dilepton signal on the reaction evolution time including the corresponding densities. Aim of this analysis is to trace the dilepton emission in time to identify the different stages and density regimes of the heavy ion collision from which dileptons originate. The study is performed for the reaction C+C at 2 AGeV.

Let us focus our discussion on the contributions of the vector mesons and the Δ resonance. The remaining contributions, π^0 and η Dalitz decays, although large, do not play a central role in the physics one aims to explore with dilepton experiments and can be viewed as some sort of standard "background". The left panel of Fig. 12 shows the dilepton multiplicities as a function of the time at which the parent particle has been created. In the right panel, the multiplicities are shown as a function of the evolution time of the heavy ion reaction. In the latter, the continuous emission of dileptons from the parent particle is explicitly shown, whereas in the former the integrated value is shown. In other words, from a particle which lives from time t_i till time t_f, dileptons are emitted with rate

$$\frac{dN^{e^+e^-}(t)}{dt} = \begin{cases} \Gamma^{e^+e^-}/\gamma & \text{for } t_i \le t \le t_f \\ 0 & \text{otherwise} \end{cases} \tag{12}$$

Here t denotes the time in the frame of the evolving system (cm frame of the nucleus-nucleus collision). The Lorentz factor γ connects a time interval in this system to the corresponding one in the rest frame of the emitting particle. For each particle, the function of t (12) is plotted in the right panel of Fig.12 and corresponds to a straight line going from t_i to t_f. The corresponding integral

$$\int_{t_i}^{t_f} \frac{dN^{e^+e^-}(t)}{dt}\, dt = \Gamma^{e^+e^-}\ \tau \tag{13}$$

where $\tau = (t_f - t_i)/\gamma$ is the life-time of the particle, gives the total number of dilepton emitted by the particle (created at $t = t_i$) and is reported in the left panel of Fig.12.

We observe that:

- Most dileptons originate from particles created within the first 8 fm. The emission is maximal from vector mesons created at about 5 fm and Δ resonances created at slightly earlier time (about 3.5 fm). This is understandable if one considers that in the resonance model vector mesons arise from the decay of baryonic resonances. Since the baryonic resonances have a typical total width of the order of 100-200 MeV, their decay takes typically place about 1-2 fm after their creation.

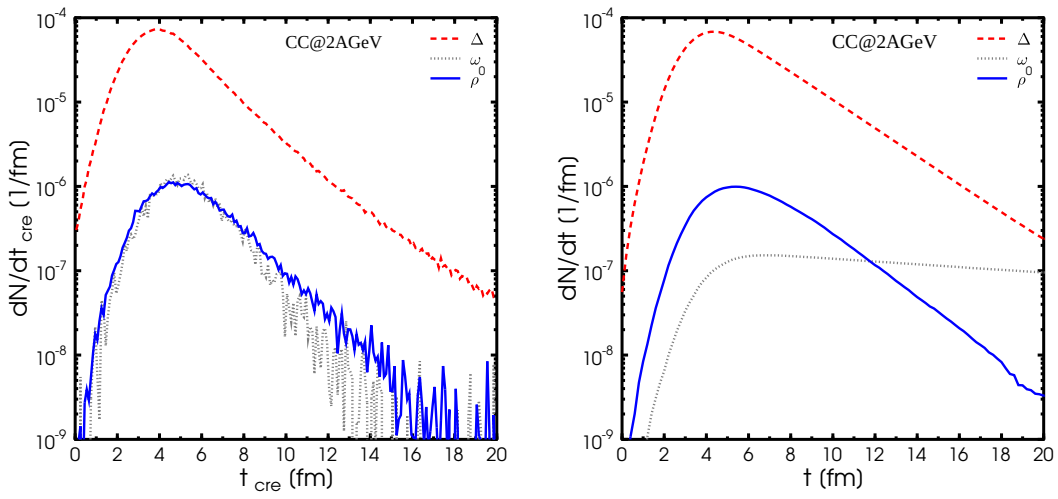

FIG. 12: (Color online) Dilepton multiplicity for minimal bias C+C collisions at beam energies of 2 AGeV as a function of the time at which the parent particle made its first appearance in the evolving system (left panel) and corresponding averaged dilepton rate as a function of the evolution time of the heavy ion collision (right panel).

- In the case that the parent particles is a relatively short lived particle, e.g. a Δ-resonance or a ρ meson, most dileptons are emitted within the first 10 fm, with a maximum around 6 fm. Later, for $t > 6$ fm, the dilepton emission strongly decreases with increasing time. On the contrary, if the parent particles is a long lived particle, e.g. a ω meson, dileptons are emitted continuously at an almost constant rate for $t > 6$ fm. This is due to the fact that those ω mesons which happened to survive the various absorption processes live relatively long and emit dileptons during their whole life-time.

In Fig. 13 the role of absorption on the reduction of the dilepton signal is shown. The observed yield is compared to the yield expected from a vacuum-like picture in which the parent resonance, after being produced, does not interact further up to its decay, here simply denoted by "full weight" scenario. For a detailed discussion of the different prescriptions for dilepton production see [24]. The total dilepton signal from vector mesons is reduced by a factor 1.5(for the ρ meson)-2(for the ω meson) due to reabsorption. Especially in the case of the ω meson the "potential" dilepton signal of those particles which are absorbed (labelled by $\omega_{\rm abs}$ in Fig 13) is strongly suppressed (by a factor 20).

Next, we investigate the influence of the baryon density locally present on the electromagnetic

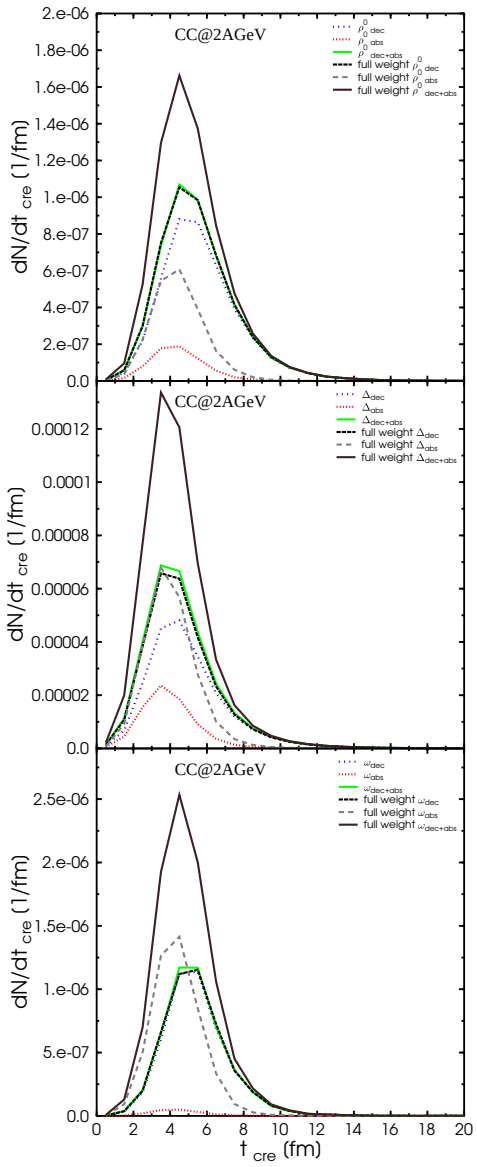

FIG. 13: (Color online) Dilepton multiplicity from minimal bias C+C collisions at beam energies of 2 AGeV as a function of the time at which the parent particle made its first appearance in the evolving system. The dashed lines denote calculation where the full branching ratio into dileptons is attached to both the decay and the absorption vertices.

response of the system, as depicted in Fig. 14. It is clear that a particle propagating through a high density zone of the system will interact, with a certain probability, with the particles present in its surroundings. Absorptive interactions, e.g. $\rho N \rightarrow N^*(1520)$, will lead to the disappearance of the parent particle from the system within shorter times than its vacuum mean lifetime (determined by its decay width). As a consequence of its shorter lifetime, the total dilepton yield from the

particle will be reduced with respect to the yield expected if the particle would be present in the system until its decay and emit dileptons for a time interval τ_{dec}. In particular, the number of dileptons expected to be emitted by a parent particle created in a space-time point characterised by a local baryon density ρ_{cre} is analysed. The result is reported in Fig.15.

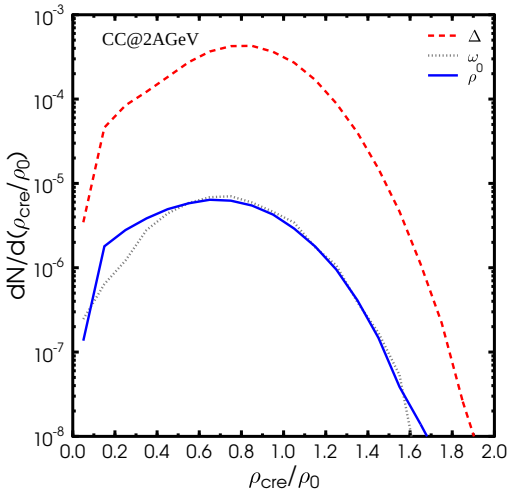

FIG. 14: (Color online) Dilepton multiplicity from minimal bias C+C collisions at beam energies of 2 AGeV as a function of the local density present in the space-time point at which the parent particle has been created.

We observe that between 13% and 20% of dileptons originate from particles created at densities $\rho_{cre} > \rho_0$ and that absorption reduces the potential dilepton yield from these particles by a factor 1.5. This effect is particularly strong in the case of the ω meson. It is evident from the previous analysis that the parent particles seem to be characterised by relatively short lifetimes in the high density phase.

VII. SUMMARY AND CONCLUSION

Dilepton production in nucleus-nucleus and proton-proton reactions at SIS/BEVELAC energies has been analysed within the microscopic transport model UrQMD. The results for invariant mass differential dilepton spectra have been compared to HADES data for C+C collisions at 1 AGeV and 2 AGeV and to DLS data for *pp* reactions. Additionally, predictions for dilepton spectra in *pp* reactions at 1.25 GeV, 2.2 GeV and 3.5 GeV as well as in Ar+KCl at 1.78 AGeV have been

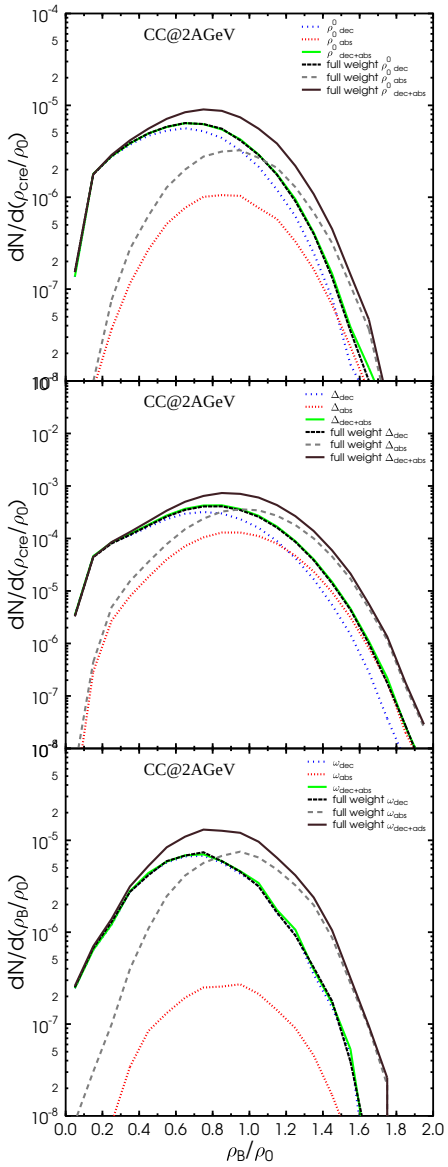

FIG. 15: (Color online) Dilepton multiplicity from minimal bias C+C collisions at beam energies of 2 AGeV as a function of the local density present in the space-time point at which the parent particle has been created. The dashed lines denote calculation where the full branching ratio into dileptons is attached to both the decay and the absorption vertices.

presented. The analysis shows that the low mass region of the dilepton spectra for C+C collisions is slightly underestimated by the model calculations at 1 AGeV, but well described at 2AGeV.

The dilepton emission was analyzed in dependence of the evolution time and densities typical for the regime probed by the HADES experiment. In particular, the influence of absorption of the parent resonances on their dilepton emission has been discussed. We found that absorption is

responsible for a global suppression of the dilepton signal of about a factor 1.5-2. The absorption processes are more copious in the high density phase, resulting in a stronger suppression for particles (and therefore dileptons) produced at the highest densities.

VIII. ACKNOWLEDGEMENTS

We thank Y. Pachmayer for providing the experimental data and the HADES filter for the reaction C+C at 1 AGeV, and E. L. Bratkovskaya for discussions on the ρ meson production cross section. This work was supported by BMBF, GSI and the Hessen Initiative for Excellence (LOEWE) through the Helmholtz International Center for FAIR (HIC for FAIR).

[1] M. A. Mazzoni [HELIOS/3 Collaboration.], Nucl. Phys. A **566**, 95C (1994); M. Masera [HELIOS Collaboration], Nucl. Phys. A **590**, 93C (1995).

[2] G. Q. Li and C. M. Ko, Nucl. Phys. A **582**, 731 (1995).

[3] G. Agakishiev *et al.* [CERES Collaboration], Phys. Rev. Lett. **75**, 1272 (1995); A. Drees, Nucl. Phys. A **610**, 536C (1996).

[4] G. Q. Li, C. M. Ko and G. E. Brown, Phys. Rev. Lett. **75**, 4007 (1995).

[5] R. Rapp, G. Chanfray and J. Wambach, Phys. Rev. Lett. **76**, 368 (1996); R. Rapp and J. Wambach, Adv. Nucl. Phys. **25**, 1 (2000).

[6] C. M. Ko, G. Q. Li, G. E. Brown and H. Sorge, Nucl. Phys. A **610**, 342C (1996).

[7] G. Q. Li, C. M. Ko, G. E. Brown and H. Sorge, Nucl. Phys. A **611**, 539 (1996).

[8] R. Rapp, G. Chanfray and J. Wambach, Nucl. Phys. A **617**, 472 (1997).

[9] B. Friman and H. J. Pirner, Nucl. Phys. A **617**, 496 (1997).

[10] W. Cassing, E. L. Bratkovskaya, R. Rapp and J. Wambach, Phys. Rev. C **57**, 916 (1998).

[11] R. J. Porter *et al.* [DLS Collaboration], Phys. Rev. Lett. **79**, 1229 (1997).

[12] E. L. Bratkovskaya, W. Cassing, R. Rapp and J. Wambach, Nucl. Phys. A **634**, 168 (1998).

[13] C. Ernst, S. A. s, M. Belkacem, H. Stoecker and W. Greiner, Phys. Rev. C **58**, 447 (1998).

[14] K. Shekhter, C. Fuchs, A. Faessler, M. Krivoruchenko and B. Martemyanov, Phys. Rev. C **68**, 014904 (2003).

[15] R. Arnaldi *et al.* [NA60 Collaboration], Phys. Rev. Lett. **96**, 162302 (2006).

[16] D. Adamova *et al.*, Phys. Lett. B **666**, 425 (2008).

[17] G. Agakichiev *et al.* [HADES Collaboration], Phys. Rev. Lett. **98**, 052302 (2007).

[18] G. Agakishiev *et al.* [HADES Collaboration], Phys. Lett. B **663**, 43 (2008).

[19] M. D. Cozma, C. Fuchs, E. Santini and A. Fassler, Phys. Lett. B **640**, 170 (2006).

[20] D. Schumacher, S. Vogel and M. Bleicher, Acta Phys. Hung. A **27**, 451 (2006).

[21] M. Thomere, C. Hartnack, G. Wolf and J. Aichelin, Phys. Rev. C **75**, 064902 (2007).

[22] J. Ruppert, C. Gale, T. Renk, P. Lichard and J. I. Kapusta, Phys. Rev. Lett. **100**, 162301 (2008).

[23] E. L. Bratkovskaya and W. Cassing, Nucl. Phys. A **807**, 214 (2008).

[24] S. Vogel, H. Petersen, K. Schmidt, E. Santini, C. Sturm, J. Aichelin and M. Bleicher, Phys. Rev. C **78**, 044909 (2008).

[25] E. Santini, M. D. Cozma, A. Faessler, C. Fuchs, M. I. Krivoruchenko and B. Martemyanov, Phys. Rev. C **78**, 034910 (2008).

[26] G. E. Brown and M. Rho, Phys. Rev. Lett. **66**, 2720 (1991).

[27] T. Hatsuda and S. H. Lee, Phys. Rev. C **46**, 34 (1992).

[28] W. Peters, M. Post, H. Lenske, S. Leupold and U. Mosel, Nucl. Phys. A **632**, 109 (1998); M. Post, S. Leupold and U. Mosel, Nucl. Phys. A **689**, 753 (2001); M. Post, S. Leupold and U. Mosel, Nucl.

Phys. A **741**, 81 (2004).

[29] M. F. M. Lutz, G. Wolf and B. Friman, Nucl. Phys. A **706**, 431 (2002) [Erratum-ibid. A **765**, 431 (2006)].

[30] J. Aichelin and H. Stöcker, Phys. Lett. **B176**, 14 (1986); H. Sorge, H. Stöcker, and W. Greiner, Annals of Physics **192**, 266 (1989); J. Aichelin, Phys. Rep. **202**, 233 (1991).

[31] S. A. Bass, C. Hartnack, H. Stöcker, and W. Greiner, Phys. Rev. **C51**, 3343 (1995).

[32] L. A. Winckelmann *et al.*, Nucl. Phys. A **610**, 116c (1996).

[33] C. Sturm *et al.* [KaoS Collaboration], Phys. Rev. Lett. **86** 39 (2001).

[34] S. A. Bass *et al.*, Prog. Part. Nucl. Phys. **41**, 225 (1998).

[35] M. Bleicher *et al.*, J. Phys. G **25** 1859 (1999).

[36] H. Petersen, M. Bleicher, S. A. Bass and H. Stocker, arXiv:0805.0567 [hep-ph].

[37] L. A. Winckelmann, H. Sorge, H. Stöcker, and W. Greiner, Phys. Rev. **C51**, R9 (1995).

[38] W. M. Yao *et al.* [Particle Data Group], J. Phys. G **33**, 1 (2006).

[39] R. Holzmann *et al.* [TAPS Collaboration], Phys. Rev. C **56**, 2920 (1997).

[40] H. Calen *et al.*, Phys. Rev. C **58**, 2667 (1998).

[41] S. Teis, W. Cassing, M. Effenberger, A. Hombach, U. Mosel and G. Wolf, Z. Phys. A **356**, 421 (1997).

[42] R. Averbeck *et al.* [TAPS Collaboration], Z. Phys. A **359** (1997) 65.

[43] L. G. Landsberg, Phys. Rept. **128**, 301 (1985).

[44] P. Koch, Z. Phys. C **57**, 283 (1993).

[45] A. Faessler, C. Fuchs and M. I. Krivoruchenko, Phys. Rev. C **61**, 035206 (2000).

[46] G. Wolf, G. Batko, W. Cassing, U. Mosel, K. Niita and M. Schaefer, Nucl. Phys. A **517**, 615 (1990)

[47] E. L. Bratkovskaya, W. Cassing, M. Effenberger and U. Mosel, Nucl. Phys. A **653**, 301 (1999).

[48] U. W. Heinz and K. S. Lee, Nucl. Phys. A **544**, 503 (1992).

[49] W. K. Wilson *et al.* [DLS Collaboration], Phys. Rev. C **57**, 1865 (1998).

[50] A. Faessler, C. Fuchs, M. I. Krivoruchenko and B. V. Martemyanov, J. Phys. G **29**, 603 (2003).

[51] E. L. Bratkovskaya and C. M. Ko, Phys. Lett. B **445**, 265 (1999).

[52] L. P. Kaptari and B. Kampfer, Nucl. Phys. A **764**, 338 (2006).

[53] M. Schafer, T. S. Biro, W. Cassing and U. Mosel, Phys. Lett. B **221**, 1 (1989).

[54] R. Shyam and U. Mosel, Phys. Rev. C **67**, 065202 (2003).

[55] R. Shyam and U. Mosel, arXiv:0811.0739 [hep-ph].

[56] V. Flaminio, W. G. Moorhead, D. R. O. Morrison and N. Rivoire, Compilation of cross. sections III: p and $\bar{p}$ induced reactions, CERN-HERA 84-01 (1984).